Dosimetry of Three Cone Beam Computerized Tomography Scanners at Different Fields of View in Terms of Various Head and Neck Organs

Sima Nikneshan,[1] Mahmood Reza Aghamiri,[2] Ehsan Moudi,[3] Nika Bahemmat,[4] and Hoora Hadian[5,*]

[1]Department of Oral and Maxillofacial Radiology, Dental Faculty, Shahid Beheshti University of Medical Sciences, Tehran, Iran
[2]Department of Radiation Medicine, Shahid Beheshti University, Tehran, Iran
[3]Department of Oral and Maxillofacial Radiology, Dental Faculty, Babol University of Medical Sciences, Babol, Iran
[4]Department of Oral and Maxillofacial Radiology, Dental Faculty, Alborz University of Medical Sciences, Karaj, Iran
[5]Department of Oral and Maxillofacial Radiology, Dental Faculty, Mazandaran University of Medical Sciences, Sari, Iran

[*]*Corresponding author*: Hoora Hadian, Department of Oral and Maxillofacial Radiology, Dental Faculty, Mazandaran University of Medical Sciences, Sari, Iran. Tel: +98-1133044000, E-mail: h.haadian@yahoo.com

Abstract

Background: Marketing new radiography devices necessitates documenting their absorbed X-ray doses. Since the current literature lacks studies on new devices, we assessed the doses of two new devices that had not previously been assessed.

Objectives: The new devices were compared to the Promax three dimensional (3D) scanner at two fields of view (FOV) in nine critical head and neck tissues and organs.

Materials and Methods: Seventeen thermoluminescence dosimeters positioned in an average-sized male RANDO phantom were used to determine the dosimetry of the three cone beam computerized tomography devices (NewTom VGi, NewTom 5G, and Promax 3D) at two field of views (FOVs), one small and one large. The exposure by each device per FOV was performed five times (30 exposures). The absorbed and effective doses were calculated for the thyroid, parotid, submandibular gland, sublingual gland, calvarium, cervical vertebra, trunk of the mandible, and mandibular ramus. The doses pertaining to the different devices, the FOVs, and the tissues were compared using the Kruskal-Wallis, Mann-Whitney U, and Wilcoxon tests.

Results: The average absorbed doses, respectively, for the large and small FOVs were 17.19 and 28.89 mGy in the Promax 3D, 19.25 and 35.46 mGy in the NewTom VGi, and 18.85 and 30.63 mGy in the NewTom 5G. The absorbed doses related to the FOVs were not significantly different (P value = 0.1930). However, the effective doses were significantly greater at the smaller FOVs / higher resolutions (P = 0.0039). The doses of the three devices were not significantly different (P = 0.8944). The difference among the nine organs/tissues was significant (Kruskal-Wallis P=0.0000).

Conclusion: The absorbed doses pertaining to the devices and the FOVs were not significantly different, although the organs/tissues absorbed considerably different doses.

Keywords: Cone Beam Computed Tomography, Dosimetry, Field of View, Resolution, Absorbed Dose, Effective Dose

1. Background

Cone beam computerized tomography (CBCT) uses a collimated and cone-shaped X-ray beam rather than a larger fan or cone beam, which allows for a scan range with a more restricted field of view (FOV). The beam's cylindrical FOV may differ from small to large fields for dental imaging or other facial examinations (1-3). Some CBCT units allow for the selection of different FOVs to suit a specific purpose (3, 4). The advantages of CBCT over CT scanning include lower costs, smaller size, and a lower dose of radiation (1, 3, 5, 6). Recent technological improvements have made it more comfortable for patients to undergo a CBCT examination as well as more convenient for dentists to acquire and analyze images (7, 8). Since the technology is new and the scanners are provided by different manufacturers, little of the process is currently understood by most radiologists, and some concerns have arisen regarding the patient's radiation dose (9-14). Due to the hazards of X-ray irradiation, it is imperative to reduce the radiation dose given to the patient to the lowest possible amount (8, 15). The CBCT radiation dose is lower than that of a helical CT scan (8, 16, 17). However, the examination dose varies considerably when using different CBCT scanners, or when using a single CBCT unit that is configured to different settings (8, 10-14, 16).

If the dose can be changed considerably by selecting different exposure parameters, it is necessary to thoroughly understand the various options as well as their impact on radiation safety (8, 18). Moreover, technological advancements are expected to improve the efficacy of each newly introduced device, while at the same time reduc-

ing the adverse effects. Such a health precaution can be achieved via altering multiple variables such as different structures (filtration, the source-to-object distances, etc.) and different radiation protocols (kVp, mAs, and FOVs) (3, 8, 10, 16, 17, 19-22). Hence, when marketing a new model of CBCT scanner, it is necessary to document its radiation doses. Various studies have evaluated human phantoms in order to assess the radiation doses received (3, 10, 16, 17, 19-22). Of course, it is difficult if not impossible to compare the results of these studies because of methodological differences such as the number of sensors used, their types, and their positioning (23). However, to the best of our knowledge, there has been only one study involving the NewTom VGi (in 15 × 15 and 23 × 23 cm² FOVs) (23), while there has been no study concerning the radiation doses of the NewTom 5G. Therefore, we conducted this study to document the radiation doses of the NewTom VGi (in 8 × 8 and 6 × 6 cm² FOVs, none of which were documented before) and the NewTom 5G (not assessed before at any configurations) in comparison to the Promax three dimensional (3D) scanner.

CBCT volumes can vary depending on the FOVs used. Large FOVs result in volumes adequate for covering the maxillofacial area, while medium and small FOVs generate volumes more appropriate for dentoalveolar and localized imaging, respectively (1-3, 23). Some organs have higher tissue weightings, which increases the damaging impact of radiation. In the head and neck area, the thyroid, salivary glands, calvarium, mandible ramus / trunk, and cervical vertebrae are examples of such organs.

2. Objectives

This study analyzed the absorbed and effective doses of these critical organs under irradiation from two different FOVs of three CBCT scanners.

3. Materials and Methods

This in vitro experimental study was performed on the ten upper sections of an anthropometric phantom (Radiation Analogue Dosimetry System (RANDO), nuclear associates, Hicksville, NY, USA). This phantom is similar to an average-sized man in terms of tissue density and radiation absorption. It is cross-sectioned with solid sections of 2.5 cm in height. Each section has sockets for embedding dosimeters. The ethical protocols of this study (in terms of the health of the operators) were approved by the research committee of the university. All experiments were performed in accordance with the relevant X-ray safety standards. All devices used in this study were properly calibrated and their quality was assessed and approved.

3.1. Thermoluminescence Dosimeter (TLD) Calibration

A total of 20 white circular thermoluminescence dosimeters (TLD) of 0.8 mm in height and 4.5 mm in diameter ((LiF: Mg, Cu, P), TLD GR 200A, conqueror electronics technology Co. Ltd, China) were used in this study. The TLDs contain sensitive mineral crystals. The most common crystal is LiF, which has a radiation absorption capacity similar to that of human soft tissue.

Each TLD was sensitive to 1 μGy - 10 Gy doses, with a linear response curve.

Calibration was repeated prior to the examination of each of the CBCT devices as detailed below. First, the dosimeters were shipped to the dosimetry laboratory of the atomic energy organization for calibration purposes. In order to reduce the error, the element correction coefficient (ECC) was calculated for all of the dosimeters. The exposure to radiation for calibrating and ECC calculation was carried out in six separate phases at the secondary standard dosimetry laboratory (SSDL) of the atomic energy organization. The energy used for the calibration was similar for all of the TLDs and it was determined based on routine energy usage in CBCT devices. These formulae would be used again later to convert the TLD output into the absorbed dose.

3.2. TLD Loading in the Phantom

Seventeen calibrated and annealed TLDs were simultaneously positioned within the phantom in positions representative of the thyroid gland, parotid gland, submandibular gland, sublingual gland, calvarium, cervical vertebra, trunk of the mandible, and mandibular ramus (Table 1). The number of TLDs placed in each bony area was based on the relative proportion of bone marrow distributed among the different bones in the human body (Table 1) (24). The remaining three TLDs were positioned in different areas of the radiology center in order to measure the background radiation. For each imaging procedure, all of the TLDs were simultaneously loaded within the phantom. Underhill et al. (25) suggested embedding at least three dosimeters in the calvarium for the assessment of calvarial dosage. Therefore, we used four sensors so as to improve the accuracy of our tests. The lower sections of the RANDO were not used, since the dose received by the lower phantom sections is not significant in oral radiography (22).

3.3. TLD Exposure

The phantom was transferred to three private radiology centers, each of which housed a CBCT device. At each clinic, radiologists positioned the phantom in such a way to accurately resemble a human subject. The phantom was

Table 1. Positions of the Dosimeters Within the Phantom Sections

Organ	Number of Dosimeters	Depth	Phantom Slice Number
Thyroid gland	3	One in the midline (deep) and two at bilateral sides (superficial)	9 and 10
Salivary glands			
Parotid gland	2	Right and Left	6
Submandibular gland	2	Right and Left	7
Sublingual gland	1		8
Red bone marrow			
Calvarium	4	Anterior-Posterior-Left-Right	2 and 3
Cervical vertebra	1		6
Trunk of the mandible	2	Right and Left	7
Mandibular ramus	2	Right and Left	6

exposed at two different fields of view (a large and a small FOVs) ten times (i.e., five times per FOV).

The exposed area was adjusted to cover the mandible in such a way that the inferior border of the FOV was 1 cm lower than the mandibular inferior border. Also, the anterior border of the FOV was 5 mm anterior to the most prominent point of the chin.

All of the CBCT devices had passed quality control tests. The utilized devices were:

1. NewTom VGi (NewTom Inc., Verona, Italy), with a constant kVp of 110. The device automatically configured mAs based on tissue mass and density in a smart and undisclosed manner. The average mAs was measured as 6.87 and 12.24 for the large and small FOVs, respectively. The large and small FOVs were 8×8 cm^2 and 6×6 cm^2, respectively. The voxel size was 150 μm in the larger FOV. This device automatically configured the resolution at high (voxel size = 100 μm) when choosing the smaller FOV. This could not be manually reserved. However, the resolution was optional (high or normal) for the larger FOV. In order to increase the variables, we chose the normal resolution for the larger FOV.

2. NewTom 5G (NewTom Inc., Verona, Italy), with a constant kVp of 110 and automatically configured mAs. The average mAs was measured as 6.76 and 11.52 for the large and small FOVs, respectively. The large and small FOVs were 8×8 cm^2 and 6×6 cm^2, respectively. The voxel size was exactly the same as that of the VGi version. As with the above device, we manually configured the resolution at normal for the larger FOV.

3. Promax 3D (Planmeca, Helsinki, Finland), configured at standard parameters for an average mature person (kVp = 82, mA = 10, and time = 12 s). The large and small FOVs were 8×8 cm^2 and 4×5 cm^2, respectively. To render the con-

ditions similar to those of the above two devices, the resolution of this device was manually configured at high as well. Also, the resolution was manually configured at normal for the larger FOV in order to foster similarity with the other two devices.

3.4. TLD Reading

After each of the 30 exposures, the phantom and dosimeters were shipped to the TLD laboratory at the university for reading (Fimel, France). The time between each irradiation and each measurement was constant for all measurements (24 hours). The TLDs were stored at about 25°C during this time.

Once at the laboratory, the dosimeters were first extracted using a vacuum device (ETT, Fimel, France). Then, they were read (TLD reader, Fimel, France), preheated, and heated, so that the absorbed X-ray dose could be emitted as visible light. This light was read and converted to the absorbed dose using the formula obtained from the above-mentioned six-phase TLD calibration and ECC estimation procedure. Finally, using an annealing device (ETT, Fimel, France), the dosimeters were reset and calibrated for the next exposure.

3.5. Absorption and Effective Dose Estimation

The background dose was taken into account in all calculations. Since the effective dose is still considered to be the most appropriate radiation risk estimator for live tissues, it was calculated according to the formula $E = \Sigma (W_T \times H_T)$, wherein W_T is the tissue weighting factor, which according to ICRP-2007 is 0.04, 0.01, and 0.12 for the thyroid, salivary glands, and red bone marrow, respectively. H_T is the equivalent dose, calculated using the formula $H_T = \Sigma (W_R \times D_R)$, wherein D_R is the absorbed dose and W_R is the

radiation weighting factor, which is defined as 1 for X-ray. The equivalent dose of red bone marrow was calculated based on the mandibular (trunk and ramus) doses, cervical vertebral doses, and calvarial doses (16).

3.6. Statistical Analysis

Descriptive statistics were calculated for the absorbed and effective doses. The doses pertaining to the devices and the organs were compared using the Kruskal-Wallis test and a Dunn post hoc test. The small and large FOV doses were compared using the Mann-Whitney U test. The effective doses related to the large and small FOVs were compared using the Wilcoxon signed-rank test. The level of significance was predetermined as P < 0.05.

4. Results

The average absorbed doses, respectively, for the large and small FOVs were 17.19 and 28.89 mGy in the Promax 3D, 19.25 and 35.46 mGy in the NewTom VGi, and 18.85 and 30.63 mGy in the NewTom 5G (Figure 1, Table 2). The highest variation between doses received by the different organs was seen in the NewTom 5G and Promax 3D (mainly with the small FOV; Table 3). The Kruskal-Wallis test indicated a significant difference between the organ dosages measured at both FOVs together (P < 0.001; Figure 2, Table 4). The Dunn post hoc test indicated significant differences between the thyroid and the submandibular gland, the mandibular trunk, and its ramus, between the parotid and the submandibular glands, and finally between the calvarium and the submandibular gland, mandibular ramus, mandibular trunk, and bone marrow (Table 5). When comparing the radiation doses absorbed by organs at the smaller FOV, the Kruskal-Wallis test showed a significant difference among the organs (P = 0.0015; Table 4). The Dunn test only showed significant differences between the submandibular gland and the thyroid and calvarium, while the other comparisons were not significant (Table 5). When comparing organ doses at the larger FOV, a significant difference among the organs was detected by the Kruskal-Wallis test (P = 0.0027; Table 4). The Dunn test only showed significant differences between the submandibular gland and the thyroid and calvarium (Table 5).

The ratios of the absorbed doses of the NewTom VGi and NewTom 5G as compared to the Promax 3D scanner are presented in Table 6. The Kruskal-Wallis test did not detect a significant difference between the doses of the devices when both of their FOVs were combined (three variables) (P = 0.8944). When each FOV of each device was considered as a separate variable (six variables), the Kruskal-Wallis test showed a non-significant difference between
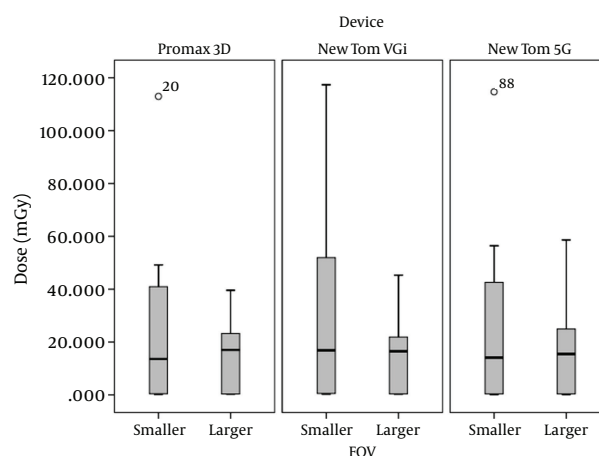

Figure 1. Boxplots of the absorbed doses per CBCT machine and FOV (CBCT, cone beam computerized tomography; FOV, field of view).
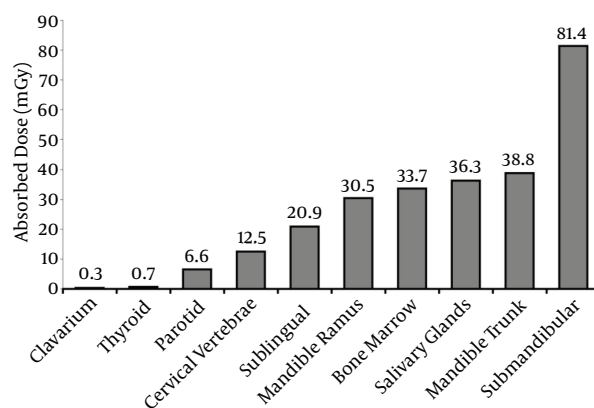

Figure 2. Absorbed doses by evaluated organs or tissues.

them (P = 0.834). The Dunn post hoc test also failed to show any difference between the two FOVs of each device (all P values > 0.05) or between each pair of two sets of device-FOV variables (all P values > 0.05). The Mann-Whitney U test showed insignificant differences between the FOVs of each device: Promax 3D (P = 0.550), NewTom VGi (P = 0.291), and NewTom 5G (P = 0.535). The difference between the FOV doses was insignificant according to the Mann-Whitney U test (P value = 0.1930). The effective doses were all greater when the device was set at the smaller FOV compared to the larger FOV. This difference was statistically significant according to the Wilcoxon test (P = 0.0039; Table 7).

Table 2. The Absorbed Doses per Organ per FOV per Device

FOV Unit	Thyroid	Parotid	Submandibular	Sublingual	Calvarium					Mandible Ramus			Mandible Trunk			Cervical Vertebrae	Bone Marrow
					Ant.	Pos.	Rt	Lt	Avr.	Rt.	Lt.	Avr.	Rt.	Lt.	Avr.		
Promax 3D																	
8 × 8	0.335	8.466	39.572	22.381	0.499	0.357	0.266	0.259	0.345	20.828	23.207	22.018	27.879	27.235	27.557	14.797	19.279
4 × 5	1.625	6.997	112.962	16.730	0.439	0.300	0.280	0.236	0.314	40.952	25.187	33.070	48.028	49.191	48.610	10.431	29.226
NewTom VGi																	
8 × 8	0.379	7.795	45.293	21.915	0.503	0.280	0.268	0.257	0.327	19.466	17.788	18.627	22.519	21.411	21.965	15.180	41.727
6 × 6	0.884	7.638	117.366	19.867	0.548	0.346	0.338	0.284	0.379	49.715	39.246	44.481	57.765	51.943	54.854	13.824	59.876
NewTom 5G																	
8 × 8	0.376	5.057	58.645	24.943	0.403	0.244	0.183	0.187	0.254	20.860	24.934	22.897	27.926	25.144	26.535	12.218	18.725
6 × 6	0.806	3.613	114.689	19.694	0.384	0.223	0.183	0.191	0.245	42.564	40.948	41.756	56.427	49.734	53.081	8.575	33.246

Abbreviations: FOV, field of view; Ant., Anterior; Pos., Posterior ; Rt, Right ; Lt, Left; Avr, Average.

Table 3. Descriptive Statistics for the Average Radiation Doses (mGy) of the Three Devices and Two FOVs

FOV	Device	Mean	SD	CV (%)	Min	Max	95% CI	
Promax 3D	Both	23.04	26.49	115.0	0.31	112.96	10.80	35.28
NewTom VGi	Both	27.35	29.62	108.3	0.33	117.37	13.67	41.04
NewTom 5G	Both	24.74	28.79	116.4	0.25	114.69	11.44	38.04
Promax 3D								
8 × 8		17.19	12.81	74.5	0.34	39.57	8.83	25.56
4 × 5		28.89	35.36	122.4	0.31	112.96	5.78	51.99
NewTom VGi								
8 × 8		19.25	16.05	83.4	0.33	45.29	8.76	29.73
6 × 6		35.46	38.20	107.7	0.38	117.37	10.51	60.42
NewTom 5G								
8 × 8		18.85	18.09	96.0	0.25	58.65	7.03	30.67
6 × 6		30.63	36.83	120.2	0.25	114.69	6.57	54.69
All	Larger	15.24	14.61	95.9	0.18	58.65	10.69	19.79
All	Smaller	26.99	32.17	119.2	0.18	117.40	16.96	37.01

Abbreviations: CI, confidence interval; CV, coefficient of variation; FOV, field of view; SD, standard deviation; Min, minimum; Max, maximum.

5. Discussion

In most cases, the Promax 3D scanner showed lower doses compared to the NewTom VGi (and compared to the NewTom 5G in the case of a few organs). The NewTom 5G scanner showed better results than its predecessor model. The radiation generated by all three devices (with a few exceptions) was slightly lower when absorbed by the parotid and sublingual glands and the cervical vertebrae. The absorbed dose of the calvarium was similar between the large and small FOVs when generated by the NewTom 5G. It was slightly lower and greater, respectively, when the Promax 3D and NewTom VGi were tested. The rest of the organs had much higher absorbed doses (1.5 to 5 times greater) when the device, regardless of its brand / model, was configured to use the small FOV. The average doses generated by the three devices did not differ from each other. The

Table 4. Average Absorbed Doses (mGy) by Organs per both FOVs, Larger FOVs, and Smaller FOVs

Organ (FOV)	Mean	SD	CV (%)	Min	Max	95% CI	
Both							
Thyroid	0.73	0.50	67.7	0.34	1.63	0.21	1.26
Parotid	6.59	1.87	28.3	3.61	8.47	4.63	8.56
Submandibular	81.42	37.33	45.9	39.57	117.40	42.24	120.60
Sublingual	20.92	2.81	13.4	16.73	24.94	17.97	23.87
Salivary Glands	36.31	11.50	31.7	23.47	48.29	24.24	48.38
Calvarium	0.31	0.05	16.8	0.25	0.38	0.26	0.37
Mandible Ramus	30.47	10.95	35.9	18.63	44.48	18.98	41.97
Mandible Trunk	38.77	14.95	38.6	21.97	54.85	23.07	54.46
Cervical Vertebrae	12.50	2.61	20.9	8.58	15.18	9.77	15.24
Bone Marrow	33.68	15.51	46.0	18.73	59.88	17.41	49.95
Larger							
Thyroid	0.36	0.02	6.8	0.34	0.38	0.30	0.42
Parotid	7.11	1.81	25.4	5.06	8.47	2.62	11.59
Submandibular	47.84	9.79	20.5	39.57	58.65	23.52	72.15
Sublingual	23.08	1.63	7.1	21.92	24.94	19.03	27.13
Calvarium	0.31	0.05	15.6	0.25	0.35	0.19	0.43
Mandible Ramus	21.18	2.26	10.6	18.63	22.90	15.58	26.78
Mandible Trunk	25.35	2.98	11.7	21.97	27.56	17.96	32.75
Cervical Vertebrae	14.07	1.61	11.4	12.22	15.18	10.06	18.07
Bone Marrow	26.58	13.12	49.4	18.73	41.73	-6.02	59.18
Smaller							
Thyroid	1.11	0.45	40.9	0.81	1.63	-0.02	2.23
Parotid	6.08	2.16	35.6	3.61	7.64	0.71	11.46
Submandibular	115.00	2.22	1.9	113.00	117.40	109.50	120.50
Sublingual	18.76	1.76	9.4	16.73	19.87	14.38	23.14
Calvarium	0.31	0.07	21.4	0.25	0.38	0.15	0.48
Mandible Ramus	39.77	5.96	15.0	33.07	44.48	24.97	54.57
Mandible Trunk	52.18	3.22	6.2	48.61	54.85	44.19	60.17
Cervical Vertebrae	10.94	2.66	24.3	8.58	13.82	4.33	17.56
Bone Marrow	40.78	16.66	40.9	29.23	59.88	-0.60	82.16

Abbreviations: CI, confidence interval; CV, coefficient of variation; FOV, field of view; SD, standard deviation; Min, minimum; Max, maximum.

non-parametric evaluation of the FOVs also showed no significant differences between the doses caused by the large and small FOVs. However, the effective doses were considerably affected by the FOVs, with the smaller FOVs causing greater effective doses. This surprising finding is unlikely to be an artifact, since the experiment settings were controlled very carefully.

Moreover, the trends of dose increase / decrease consis-

tently changed from organ to organ in the case of all three devices. Among the evaluated organs, the calvarium and submandibular gland received the lowest and highest absorbed doses, respectively. Based on these results, it can be suggested that reducing the FOV for the sake of lowering the patient's received dose, if it accompanies an automatic resolution increase, is not a very effective method. The submandibular gland received a much higher dose compared

Table 5. Results of the Dunn Post Hoc Test Comparing the Organ Dosages[a]

Compared Organs (FOV)	P Value
Both	
Thyroid vs. Submandibular	< 0.001
Thyroid vs. Mandible Trunk	< 0.05
Thyroid vs. Bone Marrow	< 0.05
Parotid vs. Submandibular	< 0.01
Submandibular vs. Calvarium	< 0.001
Sublingual vs. Bone Marrow	> 0.05
Calvarium vs. Mandible Ramus	< 0.01
Calvarium vs. Mandible Trunk	< 0.01
Calvarium vs. Bone Marrow	< 0.01
Smaller	
Thyroid vs. Submandibular	< 0.05
Submandibular vs. Calvarium	< 0.01
Larger	
Thyroid vs. Submandibular	< 0.05
Submandibular vs. Calvarium	< 0.05

[a]Only significant comparisons are listed. All other comparisons were insignificant (P > 0.05).

to all the other organs. This necessitates protecting this particular organ during CBCT scanning. By reducing the FOV and increasing the resolution, the parotid radiation dose was reduced by about 20% in the case of the Promax 3D scanner, 3% in the case of the NewTom VGi, and 30% in the case of the NewTom 5G. This might be attributed to the location of the parotid and the fact that the focus of imaging was on the anterior mandible region, which might lead to a reduction in the parotid dose in line with the reduction of the FOV and not an increase together with the increase in resolution. This did not occur in the other salivary glands, and all salivary glands together showed about a 1.5 fold increase when the FOV was reduced and the resolution was increased. Decreasing the FOV and increasing the projections led to small changes in the calvarium dose in the Promax 3D scanner (3%) and the NewTom VGi (1%), although there were no changes in the NewTom 5G. The reason for this might be the distance of the calvarium from the region of interest, which reduced both its received dose and the changes in it. The reason for the smaller calvarium dose received in the NewTom 5G compared to the other two scanners might be the position of the patient, since the patient stands during imaging in the NewTom VGi and Promax 3D, but acquires a supine position in the NewTom 5G. The latter may place the calvarium at a farther distance from the region of interest and so expose it to less reflected radiation.

Unlike the calvarium, the mandible ramus and its body showed a considerable increase in received dose after decreasing the FOV and increasing the resolution. The mandible ramus showed the highest increase in the case of the NewTom VGi scanner (about 2.2 fold) when compared to the other two (about 1.5 to 1.6 fold). Similar increases was observed in the case of the mandible body: the NewTom VGi scanner showed a 2.4 fold increase, while other two showed 1.8 to 1.9 fold increases. Similar to the parotid, which showed a decrease when decreasing the FOV, the vertebrae also received about 10% to 30% less radiation when the FOV was reduced. The reason for this might again be their distance from the region of interest.

To the best of our knowledge, no study to date has statistically compared the radiation doses of different FOVs and different organs. All of the previous studies have been limited to cataloguing the doses. In a study performed by Palomo et al. in 2008 (14), the doses received to the head and neck organs (esophagus, midline thyroid, mandible body, submandibular, center c spine, midbrain, and orbital surface) from the CBCT (CB MercuRay) scanner in different FOVs of 6, 9 and 12 inches were examined. The average dose absorbed by the thyroid gland, mandible body on the right and left sides, submandibular gland on the right and left, and the vertebrae were 40.8, 70.6, 30.6, 60.7, 30.7, and 93.5 mGy, respectively. The average absorbed dose received by the thyroid gland from all three CBCT devices investigated in this study when in the normal mode was greater, with doses of 0.335, 0.376, and 0.379 mGy, respectively, in the case of the Promax 3D, New Tom VGi, and New Tom 5G at FOVs of 8 × 8. The difference between studies might be related to differences in exposure configurations (Kvp = 120 and mA = 15) and FOV sizes, with the FOV being 12 inches in the previous study. Also, Palomo et al. concluded that alongside decreasing the FOV, the absorbed dose reduces. They stated that the reduction in dose is greater if the organ is farther from the direct radiation beam, which is similar to our findings (14).

In a study conducted in 2008 by Hirsch et al. (3), the doses absorbed by the head and neck organs and generated by two different CBCT scanners at different FOVs and protocols were examined for the anterior region of the jaws. The average dose absorbed by the parotid gland from the Vera View 3D scanner in the case of FOVs of 4 × 8 and 4 × 4 were 2.49 and 2.22 mGy, respectively, while for the Accuitomo scanner in the case of FOVs of 6 × 6 and 4 × 4, the absorbed doses were 2.24 and 1.26 mGy, respectively. The radiation absorbed by the parotid gland was about 2 to 4 times greater in the present study compared to those results (3). Hirsch et al. also evaluated the absorbed dose of bone marrow, which was lower than that observed in

Table 6. The Ratios of the NewTom Dosages to the Promax Dosage[a]

Unit (FOV)	Thyroid	Parotid	Submandibular	Sublingual	Calvarium	Mandible Ramus	Mandible Trunk	Cervical Vertebrae	Bone Marrow
NewTom VGi									
Larger	1.13	0.92	1.14	0.98	0.95	0.85	0.80	1.03	2.16
Smaller	0.54	1.09	1.04	1.19	1.21	1.35	1.13	1.33	2.05
NewTom 5G									
Larger	1.12	0.60	1.48	1.11	0.74	1.04	0.96	0.83	0.97
Smaller	0.50	0.52	1.02	1.18	0.78	1.26	1.09	0.82	1.14

[a] Ratios greater than 1 indicate the lower dose of the Promax 3D.

Table 7. Effective Doses of the Thyroid, Salivary Glands and Red Bone Marrow[a]

Unit	FOV, cm²	Effective Dose, msv	S/L
Thyroid			
Promax 3D	(8 × 8)	0.013	4.9
Promax 3D	(4 × 5)	0.065	
NewTom VGi	(8 × 8)	0.015	2.3
NewTom VGi	(6 × 6)	0.035	
NewTom 5G	(8 × 8)	0.015	2.2
NewTom 5G	(6 × 6)	0.032	
Salivary glands			
Promax 3D	(8 × 8)	0.234	1.9
Promax 3D	(4 × 5)	0.455	
NewTom VGi	(8 × 8)	0.250	1.9
NewTom VGi	(6 × 6)	0.482	
NewTom 5G	(8 × 8)	0.295	1.6
NewTom 5G	(6 × 6)	0.459	
Red bone marrow			
Promax 3D	(8 × 8)	2.313	1.5
Promax 3D	(4 × 5)	3.507	
NewTom VGi	(8 × 8)	5.007	1.4
NewTom VGi	(6 × 6)	7.185	
NewTom 5G	(8 × 8)	2.247	1.8
NewTom 5G	(6 × 6)	3.989	

Abbreviations: S/L, the ratio of the smaller-to-larger FOV effective doses.
[a] A ratio greater than 1.0 indicates a higher effective dose caused by the smaller FOV.

this study. The reason for the higher doses observed in this study compared to the study of Hirsch et al. (3) could be the larger FOVs and higher resolutions adopted in this research, in addition to the differences in their scanner settings (kvp = 80 and mA = 5) (3).

Suomalainen et al. (26) evaluated the absorbed dose of the head and neck organs in terms of four CBCT scanners and two MDCT scanners. Their results pertaining to the Promax 3D scanner at a FOV of 8 × 5 were lower in the case of the submandibular and sublingual glands, calvarium, vertebrae, and mandible ramus and body (26). However, their result was higher in the case of the parotid. The reason for the lower doses observed in the submandibular and sublingual glands in their study (26) might be their smaller FOV. However, it was interesting that despite their smaller FOV, the parotid dose observed was higher than that in our study. A probable reason for this finding might be the differences in the positioning of the TLDs and their levels. Indeed, as Pauwels et al. (23) concluded, a slight change in exposure settings, size of FOV, the location of the dosimeters and patient, and a slight shift in the FOV of a few centimeters can notably alter the radiation received by the dosimeters (23).

It should be noted that comparing the performance of devices based solely on dosimetric studies is not possible. The purpose of dosimetry comparisons is not to determine a better device, and diagnostic needs dictate the extent of necessary doses. Due to the availability of various FOV sizes in dental CBCT, as well as various positions of FOVs within the head and neck region, each point around the main beam can show high variability on the basis of its position relative to the isocenter (23). Using the same phantom allows for the dosimetric comparison of different CBCT units and different FOVs. This technique has proved reproducible, although some dosimeter locations might have some degree of variation, such as those placed close to the cranial and caudal ends of the X-ray beam, as well as those close to the skin, thyroid, and back of the neck. Hence, patient position can also alter the dose of the head and neck organs such as the thyroid. In order to reduce this, the use of smaller FOVs is suggested, which might significantly reduce the dose (10, 23). Since the absorbed dose is an average value, the only way to improve

the accuracy of dosimetry is to use as many TLDs as possible. In order to ensure the precision of the measurements in the present study, numerous TLDs were placed throughout the head and neck area to cover the head and neck organs. Still, these results should be cautiously compared with those of other studies, since the number of TLDs and their positions differ in all studies, especially as many prior studies have used too few TLDs (3, 10, 11, 16, 19, 21, 23). Utilizing too few TLDs might result in either the overestimation or underestimation of such positioning alterations, with variations of up to 80%. This can become more vivid in the case of certain tissues such as the red bone marrow, thyroid, and salivary glands (23). Such excessive variations in the doses received by each organ, as caused by different cone beam collimations and exposure factors, imply that the average effective doses should not be used for comparisons between different radiographic techniques. Still, it seems that the CBCT dose is higher than that involved in plain dental radiographic techniques, while still being below that of multi-slice CT methods (16, 17, 23). This can be increased by increasing the mAs and kV and using a larger FOV (23).

Depending on the collimation features, maximum FOV, and the quality of the diagnostic image, CBCT units could be applied for different purposes (3, 9, 16, 17, 23). Hence, an important factor when optimizing the radiation dose is to ensure the proper quality of the produced image by employing appropriate protocols such as the proper size and position of the FOV (9, 23). The ALARA principle dictates the usage of strategies to lower the radiation dose to that which is reasonably achievable (14, 19, 27) by choosing the most appropriate settings, FOV, and adequate lead protection (14). Decreasing the FOV as a collimation method is one of the approaches suggested to reduce the radiation dose. The choice of FOV should be the smallest option that would capture a given region of interest (8, 14). It is observed that reducing the size of the FOV can reduce the radiation dose (8). Therefore, it is recommended to reduce the FOV when the lesions are limited to one jaw in order to reduce the absorbed dose. However, in this study, reducing the FOV did not reduce the absorbed dose, although it did increase the effective dose. One justification for this could be the higher resolutions accompanying the smaller FOVs. Both NewTom scanners automatically adjust the resolution to a higher level when a smaller FOV is selected, and they do not allow for manual correction of the resolution modification. We also manually simulated this reverse resolution FOV association of the NewTom devices on the Promax 3D device. A higher resolution increases the radiation dose (8). It is possible that the devices are designed this way in order to improve the signal-to-noise ratio with a higher resolution. Still, this strategy contradicts the philosophy

of reducing the FOV for the sake of reducing the dose. Usually, offering many options for the operator to manually change the device's settings is not practical and so it might actually be desirable to have fewer (but less confusing) options. However, manufacturers are also suggested to let the operator have a minimum of control over the configurations. If a greater resolution is needed for a particular diagnostic task, it is important that the signal-to-noise ratio is adequate for the task. The worst form of excess exposure is a level too low to provide adequate image quality, which necessitates a repeat. However, there might be instances where a smaller FOV with a lower resolution suffices for adequate image quality. As we wanted to make the groups uniform, the Promax 3D scanner, which allowed manual resolution adjustment, was manually configured at its high resolution option for the smaller FOV. The Promax 3D has three levels of resolution. The high and normal resolutions employ the same exposure parameters, while the low resolution might reduce the effective dose to about 10% of the normal dose resolution. Generally, a low dose leads to an image with a low signal-to-noise ratio (8). These resolution increases might be the reason for the increases observed in the Promax 3D group when the smaller FOV was used.

This study was limited by several factors. It would have been valuable to evaluate more organs. However, it should be noted that the number of TLDs used in this study was more than the number used in many previous examinations. Additionally, due to the limited number of TLDs available as well as other technical difficulties, we were limited to disregarding some areas and focusing on more critical organs (16). As another limitation, it might be argued that the failure to match the devices' configurations might confound the results. It should be taken into account that it was impossible to match the devices, since their settings are determined by their manufacturers; therefore, all previous studies faced this issue as well. These prior studies were limited to comparing the same-name settings of different devices, without attempting to match the exposure parameters (3, 16). Furthermore, as another constraint, a CBCT study should also evaluate the quality of the image together with the extent of the absorbed doses. According to Lorenzoni et al. (22), the important factors in CBCT imaging are the size and position of the FOV and the quality of the image. The latter was not evaluated in this study, although other studies were similarly limited by this factor. Future studies should also take into account the differing qualities of the produced images. Other limitations centered on the numerous technical difficulties must be recognized, including the severe rarity of RANDO phantoms and TLDs, very high sensitivity of TLDs, difficulty of their transportation due to their very high fragility, lack of ade-

quate laboratory experts, which all made conducting this study very difficult. However, we re-performed most of the steps involved in this study from the scratch (with each step consisting of all exposures plus all calibration steps) in order to ensure the validity of the results.

While recognizing the limitations of this study, it seems that the devices did not differ considerably in terms of the generated dose. Decreasing the FOV but increasing the resolution did not reduce the absorbed dose and might actually increase the effective dose. When reducing the FOV for the sake of X-ray safety, the resolution should be taken into consideration. The risk of absorbed doses is higher in the submandibular gland, mandible trunk and ramus, and red bone marrow. In terms of the three evaluated devices, it seems that resolution might play a more important role than FOV in determining the absorbed dose of organs inside the FOV or close to it such as the thyroid gland. However, the doses absorbed by organs farther away from the FOV seem to be more affected by the size of the FOV than the resolution. The structures that are distant from the FOV (such as the calvarium) seem less likely to be affected by changes in the size of the FOV or resolution. It should be noted that without statistical comparisons, these suggestions should be considered as theorems and not as evidence. Future studies should hence conduct more experiments and perform further statistical analyses to assess these suggested theorems (28, 29).

Footnotes

Authors' Contribution: Sima Nikneshan, study conception and study design; Mahmood Reza Aghamiri: study conception and study design, Ehsan Moudi, study conception and data collection; Hoora Hadian, study conception, data collection, drafting the manuscript, and funding the study; Nika Bahemmat, drafting the manuscript.

Financial Disclosure: None declared.

Funding/Support: This study was funded by Shahid Beheshti university of medical sciences as post graduated thesis.

References

1. Sukovic P. Cone beam computed tomography in craniofacial imaging. *Orthod Craniofac Res.* 2003;**6 Suppl 1**:31–6. [PubMed: 14606532] discussion 179-82.
2. Cevidanes LH, Bailey LJ, Tucker GJ, Styner MA, Mol A, Phillips CL, et al. Superimposition of 3D cone-beam CT models of orthognathic surgery patients. *Dentomaxillofac Radiol.* 2005;**34**(6):369–75. doi: 10.1259/dmfr/17102411. [PubMed: 16227481].
3. Hirsch E, Wolf U, Heinicke F, Silva MA. Dosimetry of the cone beam computed tomography Veraviewepocs 3D compared with the 3D Accuitomo in different fields of view. *Dentomaxillofac Radiol.* 2008;**37**(5):268–73. doi: 10.1259/dmfr/23424132. [PubMed: 18606748].
4. Hamada Y, Kondoh T, Noguchi K, Iino M, Isono H, Ishii H, et al. Application of limited cone beam computed tomography to clinical assessment of alveolar bone grafting: a preliminary report. *Cleft Palate Craniofac J.* 2005;**42**(2):128–37. doi: 10.1597/03-035.1. [PubMed: 15748103].
5. Arai Y, Tammisalo E, Iwai K, Hashimoto K, Shinoda K. Development of a compact computed tomographic apparatus for dental use. *Dentomaxillofac Radiol.* 1999;**28**(4):245–8. doi: 10.1038/sj/dmfr/4600448. [PubMed: 10455389].
6. Lofthag-Hansen S, Huumonen S, Grondahl K, Grondahl HG. Limited cone-beam CT and intraoral radiography for the diagnosis of periapical pathology. *Oral Surg Oral Med Oral Pathol Oral Radiol Endod.* 2007;**103**(1):114–9. doi: 10.1016/j.tripleo.2006.01.001. [PubMed: 17178504].
7. Miracle AC, Mukherji SK. Conebeam CT of the head and neck, part 2: clinical applications. *AJNR Am J Neuroradiol.* 2009;**30**(7):1285–92. doi: 10.3174/ajnr.A1654. [PubMed: 19461061].
8. Qu XM, Li G, Ludlow JB, Zhang ZY, Ma XC. Effective radiation dose of ProMax 3D cone-beam computerized tomography scanner with different dental protocols. *Oral Surg Oral Med Oral Pathol Oral Radiol Endod.* 2010;**110**(6):770–6. doi: 10.1016/j.tripleo.2010.06.013. [PubMed: 20952220].
9. Farman AG. ALARA still applies. *Oral Surg Oral Med Oral Pathol Oral Radiol Endod.* 2005;**100**(4):395–7. doi: 10.1016/j.tripleo.2005.05.055. [PubMed: 16182157].
10. Ludlow JB, Davies-Ludlow LE, Brooks SL, Howerton WB. Dosimetry of 3 CBCT devices for oral and maxillofacial radiology: CB Mercuray, NewTom 3G and i-CAT. *Dentomaxillofac Radiol.* 2006;**35**(4):219–26. doi: 10.1259/dmfr/14340323. [PubMed: 16798915].
11. Mah JK, Danforth RA, Bumann A, Hatcher D. Radiation absorbed in maxillofacial imaging with a new dental computed tomography device. *Oral Surg Oral Med Oral Pathol Oral Radiol Endod.* 2003;**96**(4):508–13. doi: 10.1016/S1079210403003500. [PubMed: 14561979].
12. Schulze D, Heiland M, Thurmann H, Adam G. Radiation exposure during midfacial imaging using 4- and 16-slice computed tomography, cone beam computed tomography systems and conventional radiography. *Dentomaxillofac Radiol.* 2004;**33**(2):83–6. doi: 10.1259/dmfr/28403350. [PubMed: 15313998].
13. Ludlow JB, Davies-Ludlow LE, Brooks SL. Dosimetry of two extraoral direct digital imaging devices: NewTom cone beam CT and Orthophos Plus DS panoramic unit. *Dentomaxillofac Radiol.* 2003;**32**(4):229–34. doi: 10.1259/dmfr/26310390. [PubMed: 13679353].
14. Palomo JM, Rao PS, Hans MG. Influence of CBCT exposure conditions on radiation dose. *Oral Surg Oral Med Oral Pathol Oral Radiol Endod.* 2008;**105**(6):773–82. doi: 10.1016/j.tripleo.2007.12.019. [PubMed: 18424119].
15. Horner K, Islam M, Flygare L, Tsiklakis K, Whaites E. Basic principles for use of dental cone beam computed tomography: consensus guidelines of the European Academy of Dental and Maxillofacial Radiology. *Dentomaxillofac Radiol.* 2009;**38**(4):187–95. doi: 10.1259/dmfr/74941012. [PubMed: 19372107].
16. Ludlow JB, Ivanovic M. Comparative dosimetry of dental CBCT devices and 64-slice CT for oral and maxillofacial radiology. *Oral Surg Oral Med Oral Pathol Oral Radiol Endod.* 2008;**106**(1):106–14. doi: 10.1016/j.tripleo.2008.03.018. [PubMed: 18504152].
17. Loubele M, Bogaerts R, Van Dijck E, Pauwels R, Vanheusden S, Suetens P, et al. Comparison between effective radiation dose of CBCT and MSCT scanners for dentomaxillofacial applications. *Eur J Radiol.* 2009;**71**(3):461–8. doi: 10.1016/j.ejrad.2008.06.002. [PubMed: 18639404].
18. Carter L, Farman AG, Geist J, Scarfe WC, Angelopoulos C, Nair MK, et al. American Academy of Oral and Maxillofacial Radiology executive opinion statement on performing and interpreting diagnostic cone beam computed tomography. *Oral Surg Oral Med Oral Pathol Oral Radiol Endod.* 2008;**106**(4):561–2. doi: 10.1016/j.tripleo.2008.07.007. [PubMed: 18928899].

19. Tsiklakis K, Donta C, Gavala S, Karayianni K, Kamenopoulou V, Hourdakis CJ. Dose reduction in maxillofacial imaging using low dose Cone Beam CT. *Eur J Radiol.* 2005;**56**(3):413–7. doi: 10.1016/j.ejrad.2005.05.011. [PubMed: 15978765].

20. Okano T, Harata Y, Sugihara Y, Sakaino R, Tsuchida R, Iwai K, et al. Absorbed and effective doses from cone beam volumetric imaging for implant planning. *Dentomaxillofac Radiol.* 2009;**38**(2):79–85. doi: 10.1259/dmfr/14769929. [PubMed: 19176649].

21. Silva MA, Wolf U, Heinicke F, Bumann A, Visser H, Hirsch E. Cone-beam computed tomography for routine orthodontic treatment planning: a radiation dose evaluation. *Am J Orthod Dentofacial Orthop.* 2008;**133**(5):640 e1–5. doi: 10.1016/j.ajodo.2007.11.019. [PubMed: 18456133].

22. Lorenzoni DC, Bolognese AM, Garib DG, Guedes FR, Sant'anna EF. Cone-beam computed tomography and radiographs in dentistry: aspects related to radiation dose. *Int J Dent.* 2012;**2012**:813768. doi: 10.1155/2012/813768. [PubMed: 22548064].

23. Pauwels R, Beinsberger J, Collaert B, Theodorakou C, Rogers J, Walker A, et al. Effective dose range for dental cone beam computed tomography scanners. *Eur J Radiol.* 2012;**81**(2):267–71. doi: 10.1016/j.ejrad.2010.11.028. [PubMed: 21196094].

24. White SC, Rose TC. Absorbed bone marrow dose in certain dental radiographic techniques. *J Am Dent Assoc.* 1979;**98**(4):553–8. [PubMed: 285130].

25. Underhill TE, Chilvarquer I, Kimura K, Langlais RP, McDavid WD, Preece JW, et al. Radiobiologic risk estimation from dental radiology. Part I. Absorbed doses to critical organs. *Oral Surg Oral Med Oral Pathol.* 1988;**66**(1):111–20. [PubMed: 3165508].

26. Suomalainen A, Kiljunen T, Kaser Y, Peltola J, Kortesniemi M. Dosimetry and image quality of four dental cone beam computed tomography scanners compared with multislice computed tomography scanners. *Dentomaxillofac Radiol.* 2009;**38**(6):367–78. doi: 10.1259/dmfr/15779208. [PubMed: 19700530].

27. Mupparapu M. Radiation protection guidelines for the practicing orthodontist. *Am J Orthod Dentofacial Orthop.* 2005;**128**(2):168–72. doi: 10.1016/j.ajodo.2005.04.014. [PubMed: 16102399] discussion 172.

28. Nikneshan S, Mohseni S, Nouri M, Hadian H, Kharazifard MJ. The Effect of Emboss Enhancement on Reliability of Landmark Identification in Digital Lateral Cephalometric Images. *Iran J Radiol.* 2015;**12**(2):eee19302. doi: 10.5812/iranradiol.19302. [PubMed: 26060555].

29. Moshfeghi M, Taheri JB, Bahemmat N, Evazzadeh ME, Hadian H. Relationship between carotid artery calcification detected in dental panoramic images and hypertension and myocardial infarction. *Iran J Radiol.* 2014;**11**(3):eee8714. doi: 10.5812/iranradiol.8714. [PubMed: 25763086].